HOS-85-03

Pavement Texture and its Wave Scattering Properties: Application to Light Reflectance and Skid Resistance

A.L. Kazakov

Ontario

Ministry of
Transportation and
Communications

Research and
Development
Branch

86-04024/

Technical Report Documentation Page

MTC Report Number	ISBN Number	Other Document Number	Date
HOS-85-03			Dec/85

Title: Pavement Texture and its Wave Scattering Properties: Application to Light Reflectance and Skid Resistance

Author: A.L. Kazakov, Research Officer
Research and Development Branch
Ontario Ministry of Transportation & Communications

Published by: The Research & Development Branch, MTC

Abstract:

The reflectivity characteristics of a road surface are crucial to the luminance design of highway lighting systems. At present, the reflectance matrices used for design calculations are obtained by experimental procedure and they contain important information about the pavement surface texture.

This paper describes a model built upon the theory of dispersion of electromagnetic waves by random rough surfaces in a high frequency approximation, as applied to pavements. The model explains the reflectance properties of the pavements based on the statistical characteristics of the surface texture and physical properties of the pavement mix. To test the model, measurements were done on the Ontario Road Reflectance Matrix Photometer at the University of Toronto. When tested and calibrated, the model showed good agreement between predicted and measured data.

The backscattering of ultrasonic waves by pavement surfaces is discussed in terms of low frequency approximation of the theory of scattering from random rough surfaces. Simple experiments, using scale models, showed good correlation between the intensity of backscattering from the pavement surface and its skid resistance.

The models can be used to extract statistical surface texture characteristics from the experimental data for the assessment of other properties of pavements, such as skid resistance or pavement wear.

Key Words: skid resistance, surface texture, luminance, lighting design, dispersion of electromagnetic waves

Comments: Prepared for the 65th Annual Meeting of the Transportation Research Board, Washington, D.C.

Distribution:

Copyright Status: Crown Copyright

HOS-85-03

Pavement Texture and its Wave Scattering Properties: Application to Light Reflectance and Skid Resistance

A.L. Kazakov
Research Officer

Research and Development Branch

Published by:
The Research & Development Branch
Ontario Ministry of Transportation and Communications
Hon. Ed Fulton, Minister
D.G. Hobbs, Deputy Minister

Published without prejudice
as to the application of the findings.
Crown copyright reserved; however, this
document may be reproduced for non-commercial
purposes with attribution to the Ministry.

For additional copies contact:
The Editor, Technical Publications
Ministry of Transportation and Communications
1201 Wilson Avenue
Downsview, Ontario
Canada M3M 1J8
(416) 248-7226

December 1985

CONTENTS

	Page
LIST OF TABLES AND FIGURES	iii
1/ INTRODUCTION	1
2/ LUMINANCE CONCEPTS	3
3/ MEASUREMENT PROCEDURE	5
4/ DEVELOPMENT OF THE MODEL	6
5/ DISCUSSION OF RESULTS	11
5.1/ Scattering of Ultrasonic Waves	13
6/ CONCLUSIONS & RECOMMENDATIONS	15
7/ REFERENCES	27

LIST OF TABLES

Page

1. Measured Reflectance Coefficients, 30° 16

2. Calculated Reflectance Coefficients, 30° 17

3. Measured Reflectance Coefficients, 1° 18

4. Calculated Reflectance Coefficients, 1° 19

LIST OF FIGURES

1. Road Geometry 20

2. Ontario Road Reflectance Matrix Photometer 21

3. Two-Dimensional Representation of Mirror Reflection
   by Tangential Plane 22

4. Representation of Shadowing
   (a) Shadowing of the incident beam 23
   (b) Shadowing of the reflected ray 23

5. (a) Angular Characteristic of Light Scattering for
   Reflectance Angle of 30° 24

   (b) Angular Characteristic of Light Scattering for
   Reflectance Angle of 1° 25

6. Reflection of Ultrasound by Pavements of Different Roughness... 26

1/ INTRODUCTION

In "Proposed American National Standard Practice for Roadway Lighting" [1], the Illuminating Engineering Society (IES) recommended the luminance method of highway lighting design. The light reflectance properties of the pavement surface are key factors in the suggested design procedure. Reflectivity measurements made from a highway core sample are used to classify the pavement into one of four reflectivity classes. In simulating the viewing angle of the driver, measurements must be made at an angle of 1° to the core's surface. The data obtained in such measurements contain only limited information on the pavement surface texture characteristics. Measurements at this low angle of reflectance are tedious and require a laboratory setting to obtain the desired accuracy [2,3].

The use of a higher angle of reflection for the measurements simplifies the measuring procedure and, in conjunction with the developed model, enable calculation of the 1° reflectivity values with desirable accuracy. Moreover, the data from such measurements can be used to obtain other important pavement surface characteristics such as skid resistance and pavement wear.

A mathematical model, based on the theory of reflection of electromagnetic waves from random rough surfaces was developed and tested to transform the reflectivity values, measured at a large angle of reflection, and to obtain the pavement surface characteristics. This model enables one to predict the reflectivity values for different reflection angles from given statistical characteristics of the pavement surface texture.

Conversely, the model enables determination of pavement surface statistical characteristics from the reflection measurements at large angles of reflection.

This paper deals with the derivation of the model and describes the findings obtained with limited available experimental data.

The developed model can be used to:

1. estimate the statistical characteristics of pavement surface texture using the reflectance data,

2. predict the reflectivity values of a surface from given surface texture characteristics, and

3. convert the reflectivity values obtained for a high angle of reflectance to an angle of one degree, or other angles of reflection which might be more suitable for evaluation of a highway lighting installation from, for example, the point of view or angle of vision of a truck driver.

The next chapter provides information on the luminance concept of highway lighting design and the measurement parameters and procedures for total assessment of the problem. This information is necessary for comparison of experimental data with results obtained from the model.

2/ LUMINANCE CONCEPTS

The design of roadway lighting systems, based on the luminance concept, takes into account the amount of light reflected from the road surface towards the driver. This standard design procedure supersedes the well-known illuminance, or incident light design technique.

The procedure for determining the amount of light reflected by the road surface involves summing the intensity of light from each luminaire reflected by the pavement surface, towards the driver. The road geometry and pertinent notation are presented in Figure 1. A grid system is used for referencing points on the road. At each grid point the incident illumination for each luminaire, $E_{oi}(cd/m^2)$, is determined; and the contribution to total luminance by a particular luminaire, $L_i(cd/m^2)$, is calculated using:

$$L_i = E_{oi} \times q(\alpha, \beta, \gamma, \delta) \qquad (1)$$

where: q is the directional reflectance coefficient.

The value of q is a function of the angles of incidence γ and δ, and the angles of reflection α and β. These angles are defined in Figure 1.

The total luminance of the point P on the road then is:

$$L_p = \Sigma L_i \qquad (2)$$

It is assumed that the driver views straight ahead, thus the angle δ is zero degrees.

If we now consider the value of E_{oi} in terms of intensity, I_i, of the luminaire (light source) we have the following relationship:

$$E_{oi} = I_i(\phi, \gamma) \cos / D_i^2 \qquad (3)$$

where: $D_i^2 = h^2 / \cos^2\gamma$ and
ϕ, γ and h are as defined in Figure 1.

Substitution of E_{oi} and D_i into Equation 1 defines the luminance as a

product of factors which depend on the pavement reflective properties and lighting design parameters (for δ = 0 degrees):

$$L_i = q(\gamma, \alpha, \beta) \times I_i(\phi, \gamma) \times \cos^3 \gamma / h^2 \quad (4)$$

Reduced reflectance coefficient is defined as:

$$r = q(\gamma, \alpha, \beta) \cos^3 \gamma \quad (5)$$

substituting r simplifies Equation 4 to:

$$L_i = r(\gamma, \alpha, \beta) I_i(\phi, \gamma) / h^2 \quad (6)$$

and the total luminance of the point P is:

$$L_p = \Sigma r(\gamma, \alpha, \beta) I_i(\phi, \gamma) / h^2 \quad (7)$$

The Comite International d'Eclairage (CIE) has recommended and published standard reflectance tables [1]. These tables represent four standard surfaces which are currently used in highway lighting design. The tables (see Table 1) represent r values for α = 1° and δ = 0°. The actual reflectance matrices obtained from the measurement are only used to classify the pavement surface into one of the standard classes.

The value of the directional reflectance coefficient $q(\alpha, \beta, \gamma, \delta)$ for each value of the arguments depends upon the statistical properties of the surface geometry, or texture, and the effective optical properties of the pavement mix. The theory of reflection of the electromagnetic waves from the random rough surfaces can be applied to describe this dependence and to model the pavement reflectance properties for different angles of reflectance.

The statistical characteristics of a pavement surface texture are not readily available. Different experimental techniques were recently developed in order to obtain the texture characteristic used in skid prediction models. The developed model can be used to derive these characteristics from the directional reflectance coefficient measured at a high angle of light reflectance (30° in the present study). The texture characteristic thus obtained can be used to calculate the reflectance matrices for the pavement as well as other pavement properties which depend upon the texture.

3/ MEASUREMENT PROCEDURE

Measurement of the reflectance matrixes for a high angle of reflectance was done on the Ontario Road Reflectance Matrix Photometer at the University of Toronto. The standard procedure of measurement for 1° angle of reflectance is described in detail in References 3 and 4. The instrumentation was adjusted and calibrated for measurement at the 30° reflectance angle.

The experimental set-up for this measurement is shown in Figure 2. A photometer, M, measures the luminance of a sample from a constant angle of view $\alpha = 30°$. The constant intensity, I_o, light source (S) moves along a rail (AB) at a constant height, h, above the core sample. The photometer and the sample are rotated together around the axis A-A, and automatic readings of the photometer output are taken at specified angles, β, of rotation starting from 0° and up to 165°. The geometry of the instrument did not allow for measurements at $\beta = 180°$ with a 30° angle of reflection, so $\beta = 165°$ was the maximum rotation angle used in experiments [5].

The reduced reflectance coefficient r for each geometry of measurement is determined by rearranging Equation 4:

$$r = L\, h^2/I_o \qquad (8)$$

where L is luminance measured in a particular direction and h, and I_o are experimental parameters defined above. The directional reflectance coefficient, q, can then be determined as $q = r/\cos^3\gamma$.

4/ DEVELOPMENT OF THE MODEL

The solution of the problem of scattering of waves by flat rough surfaces having a texture smaller than the wavelength was given by Lord Rayleigh as early as 1896 in his classical monograph "The Theory of Sound" [6]. Later, the practical problems of radar technology (scattering of electromagnetic waves by the surface of the earth) lead to a broad attack on the problems of the scattering of electromagnetic waves by rough surfaces. The perturbation solution for a mildly sloping texture was suggested in References 7 and 8; the problem of wave scattering by a random surface with irregularities larger than the wavelength was solved by Brekhovskikh [9].

These first attacks on the problem were later extended to include cases of boundaries having finite conductivity [10], and boundaries with randomly varying impedance [11]. Later workers extended understanding towards more realistic surface textures, such as a combination of large irregularities (in comparison to wavelength) with the overlaying microtexture [12,13]. Different physical and mathematical methods were used in an effort to closely model reality and find better approximations. Monographs [14,15] present reviews of these investigations.

Similar results were obtained by investigators approaching the same problem from different physical perspectives. This paper mainly follows the works of Isakovich, Semenov and Sancer [10,13,16], which are based on one of the main approaches to the problem of scattering of waves - the Kirchgoff approximation and the Kirchgoff vector integral equation [17].

To model the scattering of the light by a pavement surface it is assumed that the surface is flat on the average and surface irregularities are much larger than the wavelength of the light, i.e., high-frequency approximation can be used. The later assumption is supported by scanning electron microscopy analysis of different road aggregate materials [18].

The pavement is assumed to be homogeneous in its constitutive properties, this assumption is based upon the work of Bass [11], who showed that for mixes with randomly distributed materials the effective value of the pertinent properties of materials can be used. In this model, estimation of the light intensity scattered into the particular direction is done, effectively, by summation of mirror reflections from each element of the

surface (see Figure 3). The value of this sum averaged over the ensemble represents the final result of the calculations.

The model takes into account the effect of shadowing of one part of the surface by another, which is important for grazing angles of scattering. In Figure 4 the effect of shadowing of the incident and reflected light is demonstrated. For surfaces with irregularities much larger than the wavelength of the light, the effect of secondary reflections is proved to be negligible .

In mathematical terms the pavement surface is represented as a realization of the random function $z = \zeta(x,y)$. The Kirchgoff approximation is used to calculate the field on the surface, $\vec{E}_s$, as the sum of the incident field, $\vec{E}_0$, and the field reflected (scattered) from the plane tangential to the surface at any given point, $\vec{E}_t$: $\vec{E}_s = \vec{E}_0 + \vec{E}_t$. The reflected component of the surface field, $\vec{E}_t$, can be presented as function of the incident field using the Fresnel reflection coefficients, M and N, which are specified below. Thus, the field on the sample surface can be calculated given the incident electric $\vec{E}_0$ and magnetic $\vec{H}_0$ fields and the effective values of material properties: dielectric constant ε and magnetic susceptibility, μ. Kirchgoff's integral is then applied to determine the field, $\vec{E}$, at the receiver from the field known on the enclosed surface. The electromagnetic field intensity, which is proportional to the square of the modulus of the electric field vector, $|\vec{E}^2|$, is then estimated and its ensemble average is the final result of the derivations.

The formulae used below are after Sancer [16]:

$$J = \langle|\vec{E}^2|\rangle = (|\vec{E}^2_0| / R_0^2) S(a_1/a_4) (|M|^2 + |N|^2) W_1 W_2 \qquad (9)$$

where: J = the ensemble average of the intensity of scattered light

R_0 = distance from source to the surface

S = scattering area of a sample

$$a_1 = 1 - \sin\gamma \cos\alpha \cos\phi + \cos\gamma \sin\alpha \qquad (10)$$

$$a_4 = \cos\gamma + \sin\alpha \qquad (11)$$

$$N = \{\varepsilon \cos\theta - \sqrt{(\mu\varepsilon - \sin^2\theta)}\} / \{\varepsilon \cos\theta + \sqrt{(\mu\varepsilon - \sin^2\theta)}\} \qquad (12)$$

$$M = \{\mu \cos\theta - \sqrt{(\mu\varepsilon - \sin^2\theta)}\} / \{\mu \cos\theta + \sqrt{(\mu\varepsilon - \sin^2\theta)}\} \qquad (13)$$

$$\cos\theta = \{(1 - \cos\alpha \sin\gamma \cos\phi + \sin\alpha \cos\gamma) / 2\}^{1/2} \quad (14)$$

θ = is the local angle of incidence

W_1 is the joint probability density function of the partial derivatives of the random function $z = \zeta(x,y)$; $W_1(\zeta_x, \zeta_y)$ is evaluated at the values of $\zeta_x = (\cos\alpha - \sin\gamma \cos\phi)/a_4$ and $\zeta_y = \sin\gamma \sin\phi/a_4$ or, in other words, for the mirror reflection of the incident light towards the receiver. The validity of Equation 9 is not limited to the normal, Gaussian, random surfaces. However, a Gaussian stationary isotropic random function is used to compare the results of the model to the experiments. Thus, the joint probabilities distribution of x and y components of the gradient of the surface $\zeta(x,y)$ -- $W_1(\zeta_x, \zeta_y)$ is normal and can be written as:

$$W_1 = (2\pi \langle\alpha^2\rangle) \exp\{-(\zeta_x^2 + \zeta_y^2) / (2 \langle\alpha^2\rangle)\} \quad (15)$$

$$\text{RMSS} = \langle\alpha^2\rangle \quad (16)$$

RMSS is the root mean square slope of the surface.

W_2 is a conditional probabilities function correcting the results for shadowing. It takes into account shadowing of the incident and reflected rays by an isotropic normally distributed surface. W_2 is the product of the probability of an incident ray hitting a given point on the surface, given a certain inclination at that point, and the probability of a ray reflected from a given point reaching the observer. These probabilities account for the non-shadowing of the incident and scattered fields by the surface.

$$\begin{aligned} W_2 &= (C_0 + 1) && \text{for } \alpha > \gamma, \text{ and } \beta = 0 \text{ or } 180 \\ W_2 &= (C_2 + 1) && \text{for } \alpha < \gamma, \text{ and } \beta = 0 \text{ or } 180 \\ W_2 &= (C_0 + C_2 + 1) && \text{in any other case} \end{aligned} \quad (17)$$

where:

$$2 C_0 = (2 |\langle\alpha^2\rangle| / \pi) \tan\gamma \exp\{- \cot^2\gamma / (2 |\langle\alpha^2\rangle|)\} - \text{erfc}\{\cot\gamma / (2 |\langle\alpha^2\rangle|)^{1/2}\} \quad (18)$$

$$2 C_2 = (2 |\langle\alpha^2\rangle| / \pi) \tan\alpha \exp\{- \cot^2\alpha / (2 |\langle\alpha^2\rangle|)\} - \text{erfc}\{\cot\alpha / (2 |\langle\alpha^2\rangle|)^{1/2}\} \quad (19)$$

where $\text{erfc}(x) = 1 - 2 / \sqrt{\pi} \int_0^x \exp(-x^2)dx$ is a well-known function of errors, see Reference 19.

The power scattered by a random rough surface in any direction can be calculated (in the high-frequency limit) if the statistical properties of the surface texture are given. To compare model results with measured pavement reflectance data, Equation 9 is rewritten as:

$$J = A \{I_0 / (4\pi R_0^2 \rho^2)\} F \exp\{-Bx\}) W_2 \quad (20)$$

where: $A = S \pi(1/\langle\alpha^2\rangle)$ (21)

$F = (a_1/a_4) (|M|^2 + |N|^2)$ (22)

$x = (2 a_1/a_4^2) - 1$ (23)

$I_0 = (4\pi R_0^2) |\vec{E}^2_0|$ (24)

$B = 1 / (2 \langle\alpha^2\rangle)$ (25)

ρ = distance from the surface to the receiver

Furthermore, considering the illuminance, E, with respect to the source intensity, I_0:

$$E = (I_0 / 4\pi R_0^2) \cos\gamma \quad (26)$$

and the relationship between field intensity and luminance, L:

$$J = L / (\rho^2) \quad (27)$$

we can derive a model for the reflectance coefficient. Using Equations 1, 5, 26 and 27, we have :

$$J = (I_0 r) / (4\pi R_0^2 \rho^2 \cos^2\gamma) \quad (28)$$

Equating 20 and 28 we get the following relationship:

$$r = A \cos^2\gamma F \exp(-Bx) W_2 \quad (29)$$

This expression explicitly defines reduced reflectance coefficients through the parameters of the physical model for every geometry.

By introducing $r' = r / \{F \cos^2\gamma\}$, Equation 29 can be rewritten in a form more suitable for further regression analysis:

$$r' = A \exp(-Bx) W_2 \quad (30)$$

Assuming that the effective values of the dielectric constant of the scattering surface material are known, the values F and x are defined for any geometry of measurements; A and B are regression parameters which depend on the texture; and W_2 is a shadowing factor, described above. As may be seen from Equations 17-19, W_2 depends on the geometry of scattering and root mean square slope of the surface texture. Using the experimental values of reduced reflectance coefficients of pavement, measured at a 30° angle of reflection, the root mean square slope of the texture and the constant A were found by an iterative least square procedure.

In the first step of iteration, the shadowing factor W_2 was assumed to be negligible ($W_2 = 1$) for the purpose of obtaining the constants, A and B, of expression 30. The shadowing correction W_2 was then estimated using the value of root mean square slope from the first iteration. Experimental data were then adjusted to eliminate the shadowing effect by multiplication of the reflectance matrix by the inverse shadowing factor. Using this technique, the process converged within three to four iterations.

The values of effective constitutive properties of the pavement mix ε and μ are localized within a narrow range. We assumed that the pavement mix was not magnetic, so magnetic permeability μ was set equal to unity. Electric susceptibility of the mix was assumed to be in a range 1.5 to 5. This estimate was considered to be correct since we were only dealing with dielectric highway core samples. To investigate the effect of change in these values on the model results, a sensitivity analysis was performed which showed that the model was not very sensitive to changes in the effective value of electric permeability within a given range. This was due (in part) to the high angle of reflection used - really, the value of $|M^2| + |N^2|$ which, depending upon the dielectric permeability ε and local angle of incidence, θ, is almost a constant for angles of incidence below about 60°. For the 30° reflection measurements local angle of incidence, corresponding to mirror reflection towards the receiver, was almost for all r-values measured below 60°.

5/ DISCUSSION OF RESULTS

Figure 5 shows the influence of the root mean square slope of the surface on its light reflectance property, r, as it is accounted for by the model. The graphs presented are based on the values of calculated reduced reflectance coefficients. These calculations were done for the case of direct and backward scattering angles $\phi = 90°$ and $-90°$, respectively. In other words, the receiver is in the plane of the incident ray and the normal to the average surface plane, $\vec{n}$. In addition, the graphs present the case of 90° scattering with the angle $\theta = 0$. The different parameters used in the calculation are given in the legend to Figure 5.

For almost flat surfaces, with a small value of RMSS ($\simeq 0.10$ to 0.25), the reflection is almost mirror-like. The reduced reflectance coefficient sharply decreases when the angles of scattering deviate from the angle of mirror reflection, equal to 30° for Figure 5a and 1° for Figure 5b. With increased surface roughness, the value of RMSS is increased and more diffuse, a broader scattering of light is observed. At the same time, with an increase in RMSS value the maximum of reduced reflection coefficient is shifted from the angle of mirror reflection to a larger angle γ and then for an angle $\phi = -90°$. Thus, a maximum reduced reflection coefficient is observed for a backscattering of light. The same effects are observed for the scattering of light in all directions. The shadowing of one part of the surface by another narrows the directional distribution of light scattering and shifts the maximum r-values towards the angle of mirror reflection.

The experimental reflectance matrix is presented in Table 1, for measurements with a 30° viewing angle. These data were used to obtain the root mean square slope of the pavement surface using the iterative regression procedure described above.

Table 2 presents the calculated r-matix for RMSS = 0.81 for comparison with the experimental data given in Table 1. The calculation of r-matrix is done for $\mu = 1$ and $\varepsilon = 2.5$. To estimate the explanatory power of the model, a correlation coefficient, R, between two sets of r-values was calculated according to Equation 31 and found equal to R = 0.99. This

high value of correlation coefficient shows that the directional variability of reduced reflectance coefficient is, to very large extent, encompassed by the developed model.

$$R = \{ \Sigma(X_i - \bar{X})(Y_i - \bar{Y}) \} / \{ \Sigma(X_i - \bar{X})^2 \, \Sigma(Y_i - \bar{Y})^2 \} \qquad (31)$$

Three core samples from the same pavement were used to observe the effect of local variations of roughness and model sensitivity. The RMSS values estimated by the model from these three sample reflectance matrices were in a narrow range between 0.79 and 0.82.

The theoretical reflectance matrix for a 1° viewing angle was then calculated using RMSS values of the surface estimated from 30° measurements. The experimental and calculated r-matrices for 1° reflection angle, α, are presented in Tables 3 and 4, respectively.

The value of the "A" coefficient of Equation 30 was calculated as a product of the value A obtained from 30 degree measurements and a correction factor. This correction factor, CF, is result of change in the value of experimental parameters - the surface area seen by the photomultiplier was different for the two sets of measurements, and it was found to be equal to CF = 7.

Comparing the predicted value with the actual data, we note the rate of change of the coefficients, with changes in $\tan\gamma$ and ϕ, is greater in the predicted matrix. As currently developed, the model considers the surface texture to be normally distributed, with no correlation between the gradient of the microsurface and the height of the microsurface. If we consider that road surfaces are worn down by travelling vehicles, we realize that there would be a greater number of horizontal planes at the top of the microsurface than at the bottom (conceptually, one might imagine a range of mountains with the tops chopped off). This implies that the distribution is skewed and a correlation may exist between the gradient and the height of the microtexture. This would increase the amount of reflection and cause less shadowing, thereby lowering the rate of change.

5.1/ Scattering of Ultrasonic Waves

The theory of wave scattering by random surfaces was first developed and applied to the scattering of sound. The wavelength of the high frequency ultrasonic waves (about 100,000 Hz) in air is larger by an order of magnitude than the root mean square height of the pavement texture. The tangential plane approximation developed above for light scattering is not applicable in this case, but the perturbation solution [6,15] can be used to obtain the directional scattering pattern of ultrasonic waves.

One of the fundamental conclusions of the perturbation theory is that the scattering of monochromatic radiation by random surfaces, considered in the Fraunhofer zone, depends upon only one harmonic of the surface continuum spectra. In other words, sound waves "see" a surface as having a periodic pattern of irregularities with one specific space frequency. By changing the direction of incident wave or viewing angle, different parts of the texture spectrum can be observed. The simple experiment described in Reference 20 verifies the results of this theory. The scattering of ultrasound can be used to obtain information on the pavement surface texture spectra. Then, by inverse Fourier analysis, a statistical height distribution of surface texture can be calculated.

Using the scale modelling equipment available at MTC, simple experiments were done to correlate the skid resistance of pavements with the intensity of ultrasound backscattering. An electric spark was used as a high intensity source of ultrasonic radiation, which was scattered from the 15 cm (6") core samples. On the receiving side, 1/4 inch microphones were used to pick up the ultrasound. The signal was amplified, the particular frequency filtered and the intensity of the filtered ultrasonic radiation measured. A detailed description of the experiments and equipment can be found in References 21 and 22.

In these trial experiments, only major changes in the surface roughness and not the fine features of the surface texture were observed. The increase in the surface roughness affects all spacial frequencies of the texture and so increases the intensity of ultrasound backscattering. Thus, a positive correlation is expected between pavement skid resistance and the intensity of backscattering.

The results of this experiment are presented in Figure 6, in which the ratio of intensity of backscattering to the intensity of incident radiation is plotted against the skid number. The two plots on the graph are for two different frequencies of ultrasound. These frequencies are actually centres of the 1/3 octave band of filtered radiation. As was expected, a definite positive correlation between backscattering and skid resistance of the pavement surfaces may be observed in the figure.

6/ CONCLUSIONS & RECOMMENDATIONS

The developed model and the experimental data obtained accurately explain observed reflectance properties of pavement. Furthermore, the results suggest that reflectance data can also be used for texture analysis. More detailed experimental investigations are needed to define the correlation between reflectance and pavement composition, as well as between the reflectance and other pavement properties which depend on the pavement texture.

Use of even higher reflection angles would permit the obtaining of more meaningful data in such experiments because the influence of shadowing at high angles has only insignificant effects on results. This would permit simplification of the model and allow the use of distribution functions other than the Gaussian without introduction of unknown errors.

The use of ultrasonic waves for investigation of the texture properties requires development of more suitable equipment than used in the present study. However, even in the simple experiments conducted, a correlation of ultrasound backscattering with skid resistance data was observed.

The results obtained in the experiments and model described suggest that a detailed analysis of the statistical properties of pavement texture is feasible by means of wave scattering experiments.

Table 1/ Measured Reflectance Coefficients (x 10^4)
30° angle of reflection

0	2	5	10	15	20	25	30	45	60	75	90	105	120	135	150	165
788	794	787	792	789	786	788	785	795	792	797	796	792	792	786	783	783
848	845	851	855	851	846	843	833	819	797	761	748	721	710	688	683	674
822	822	822	822	808	796	785	762	705	653	615	592	557	541	521	523	517
742	747	764	734	714	693	666	634	561	498	458	420	403	393	387	386	386
648	649	649	631	603	561	527	491	408	360	322	298	284	278	273	278	283
564	566	557	531	500	452	414	372	305	261	230	213	200	200	202	203	208
485	488	480	442	400	361	321	295	229	192	167	155	150	146	149	153	159
417	416	398	357	320	283	249	224	173	143	126	116	110	110	111	116	125
350	366	330	297	262	224	194	173	132	110	97	89	85	84	84	90	98
253	249	240	205	173	143	126	113	80	66	59	53	50	51	53	55	57
185	184	172	146	121	99	83	76	53	42	38	36	35	35	35	36	38
137	135	126	107	86	70	58	51	38	31	27	25	23	24	22	25	28
109	104	97	80	64	53	45	38	27	23	20	20	18	18	18	20	20
82	81	74	63	51	41	32	27	21	17	16	15	14	14	14	15	15
66	66	62	48	37	31	27	26	16	14	12	12	12	12	13	13	13
55	53	50	41	32	25	21	17									
46	44	42	25	27	21	17	15									
38	38	36	30	24	19	14	12									
31	33	30	26	20	15	12	11									
28	28	27	22	18	13	11										
24	25	23	20	16	12	10										
21	21	20	18	14	11	9										
19	19	18	16	14	10											
17	18	17	15	13	11											
15	15	15	14	11	9											
14	14	14	14	12	8											
13	14	13	13	11	8											
13	13	13	13	10												
12	12	12	12	10												

Table 2/ Calculated Reflectance Coefficients (x 10^4)
30° angle of reflection

0	2	5	10	15	20	25	30	45	60	75	90	105	120	135	150	165
741	741	741	741	741	741	741	741	741	741	741	741	741	741	741	741	741
789	789	788	786	783	779	774	769	748	727	707	690	677	667	660	655	652
800	799	797	790	778	764	747	730	676	632	599	575	560	548	541	537	535
788	778	773	754	728	698	666	636	561	508	472	449	434	425	419	416	414
761	732	719	683	640	597	557	523	443	393	360	340	327	318	312	309	307
724	669	645	591	537	490	450	417	345	301	273	255	243	235	229	225	223
682	596	557	493	440	396	360	331	270	232	208	192	181	174	168	164	162
631	508	464	404	357	319	289	264	212	181	160	146	136	129	124	120	118
492	413	380	330	290	259	233	212	170	143	125	113	104	97	93	90	88
318	274	257	224	196	174	157	142	112	92	79	70	63	58	54	52	50
217	190	179	157	138	122	109	99	77	63	52	45	40	36	33	31	30
154	137	130	114	100	88	79	72	55	44	36	31	26	24	22	20	19
114	102	97	85	74	66	59	53	41	32	26	22	18	16	14	14	13
86	78	74	65	57	51	45	41	31	24	19	16	13	11	10	9	9
66	60	58	51	44	39	35	32	23	18	14	12	10	8	7	7	6
53	48	46	40	35	31	28	25									
42	39	37	33	27	25	22	20									
35	32	30	27	23	21	18	17									
29	26	25	22	19	17	15	14									
24	22	21	19	16	14	13										
20	19	18	16	14	12	11										
17	16	15	14	12	10	9										
15	14	13	12	10	9											
13	12	11	10	9	8											
11	10	10	9	8	7											
10	9	9	8	7	6											
9	8	8	7	6												
8	7	7	6	5												
7	6	6	5	4												

Table 3/ Measured Reflectance Coefficients (x 10^4)
1° angle of reflectance

0	2	5	10	15	20	25	30	45	60	75	90	105	120	135	150	165
413	417	413	416	417	417	413	419	423	422	427	422	424	424	418	411	411
456	461	461	459	456	456	445	449	438	413	403	386	374	363	355	353	349
482	477	488	477	461	454	433	422	385	344	327	305	291	280	275	279	269
481	477	475	456	440	413	386	358	301	264	245	229	220	213	211	214	212
471	472	461	434	386	347	310	278	226	193	169	165	159	156	157	156	160
455	445	427	371	315	264	233	207	159	140	122	118	118	113	113	117	120
445	445	403	326	259	213	180	158	116	100	92	89	88	86	91	94	92
413	403	355	269	208	158	135	110	91	76	69	67	67	71	70	71	76
395	355	323	226	159	125	101	89	68	61	57	54	54	55	56	60	61
353	323	246	146	100	78	64	56	43	40	37	36	36	36	40	40	41
315	280	188	98	65	61	43	38	30	28	25	26	26	26	30	29	31
280	238	139	69	46	36	31	29	24	22	22	20	20	21	23	23	24
259	194	104	52	36	28	24	24	18	17	16	16	16	18	19	21	21
230	162	82	39	26	22	20	17	16	13	13	12	14	14	15	17	17
209	136	66	32	22	18	15	14	12	12	11	11	12	12	13	14	15
198	116	52	27	19	15	13	12									
165	101	44	22	16	12	12	10									
174	86	37	18	13	11	10	9									
166	81	32	16	12	10	9	8									
153	65	27	14	10	9	8										
144	61	25	13	10	9	7										
133	54	23	12	8	7	7										
131	49	20	11	8	7											
124	44	18	10	8	6											
120	42	17	9	7	6											
120	38	16	9	7	6											
117	34	16	8	7	6											
107	31	13	8	6												
105	29	13	7	6												

Table 4/ Calculated Reflectance Coefficients (x 10^4)
1° angle of reflectance

0	2	5	10	15	20	25	30	45	60	75	90	105	120	135	150	165
346	346	346	346	346	346	346	346	346	346	346	346	346	346	346	346	346
391	391	391	390	388	385	382	379	366	351	336	323	312	303	296	291	288
428	428	426	422	415	407	397	386	352	319	291	269	252	238	228	221	218
454	453	450	441	426	408	389	369	314	269	234	206	186	171	160	152	148
467	465	459	441	415	387	360	334	268	217	178	149	128	113	102	95	91
467	462	452	423	387	352	321	293	223	170	130	102	83	70	61	55	52
455	448	433	392	350	312	280	252	182	130	93	68	52	41	34	30	28
435	426	405	356	310	273	243	216	148	98	64	44	31	23	18	16	14
412	400	373	318	273	238	210	184	119	73	44	27	18	13	10	8	7
362	344	307	249	210	181	157	133	76	38	19	10	6	4	3	2	2
314	290	248	196	164	140	118	97	47	20	8	4	2	1	1	0	0
272	244	200	156	130	110	90	70	28	10	3	1	1	0	0	0	0
236	204	163	125	104	87	68	51	17	5	2	1	0	0	0	0	0
206	172	134	103	86	69	52	36	10	2	1	0	0	0	0	0	0
181	146	111	86	70	55	39	26	6	1	0	0	0	0	0	0	0
160	124	93	73	59	44	30	19	3	1	0						
165	101	44	22	16	12	12	10									
142	196	79	62	49	35	22	13	2	0							
127	92	68	53	41	28	17	10	1								
114	80	59	46	35	22	13	7	1								
102	70	51	40	29	18	10										
93	61	45	35	25	14	7										
85	54	40	31	21	12											
78	48	36	28	18	9											
71	43	32	24	15	8											
66	39	29	22	13	6											
61	34	26	19	11	5											
56	31	24	17	9												
52	29	21	15	8												
48	26	20	14	7												

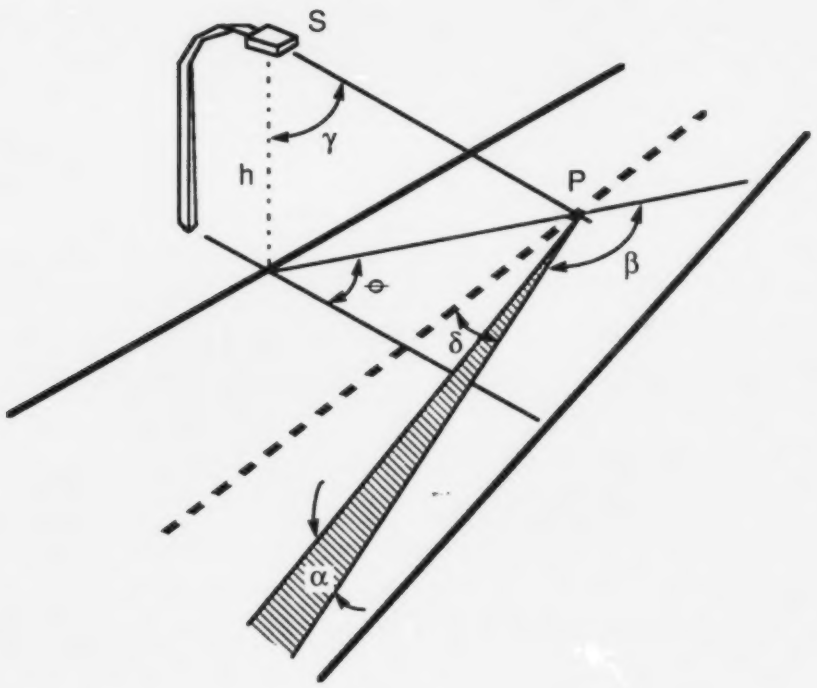

Figure 1/ Road Geometry

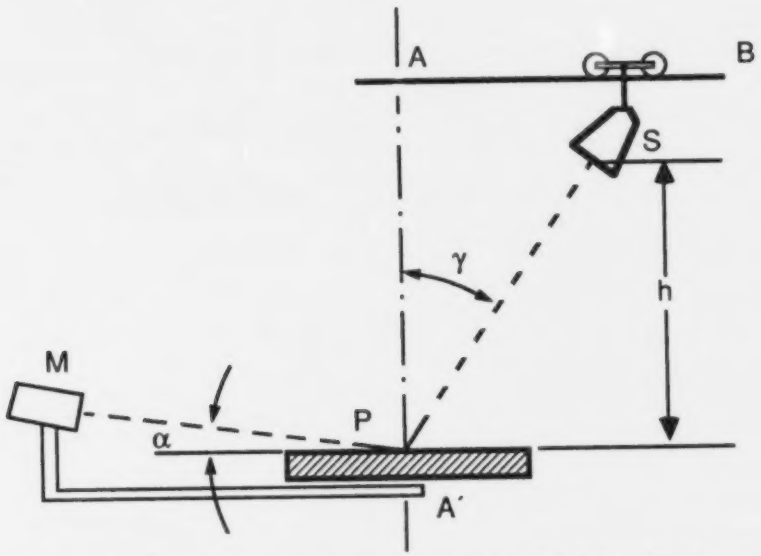

Figure 2/ Ontario Road Reflectance Matrix Photometer

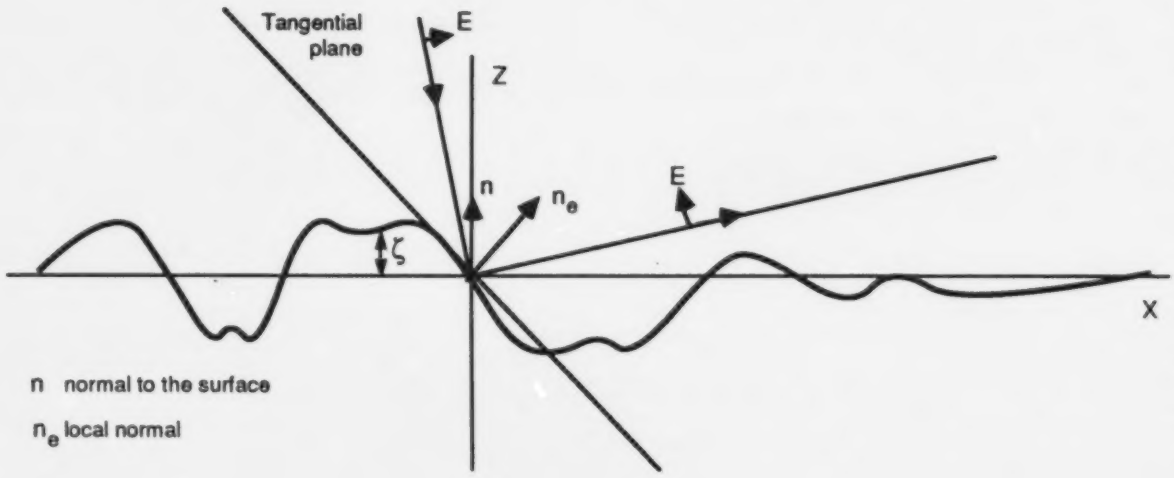

Figure 3/ Two-Dimensional Representation of Mirror Reflection by Tangential Plane

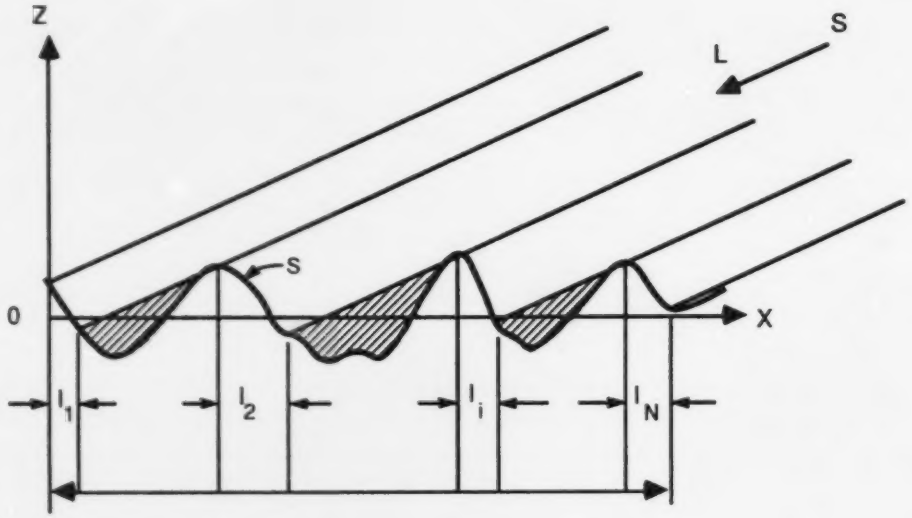

a) shadowing of the incident beam. The set $\{l_i\}$ of sample surface is illuminated by the source, S.

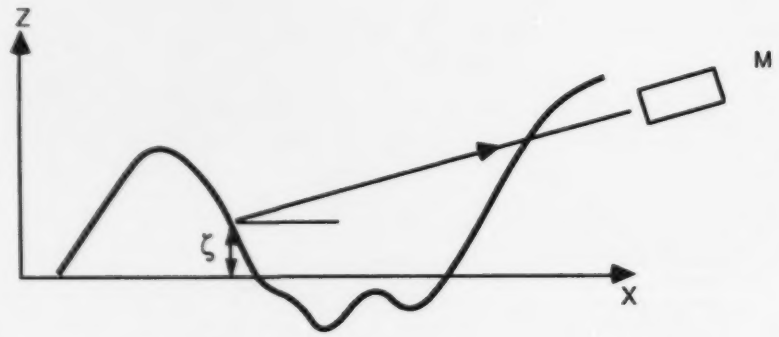

b) shadowing of the reflected ray. M is a detector.

Figure 4/ Representation of Shadowing

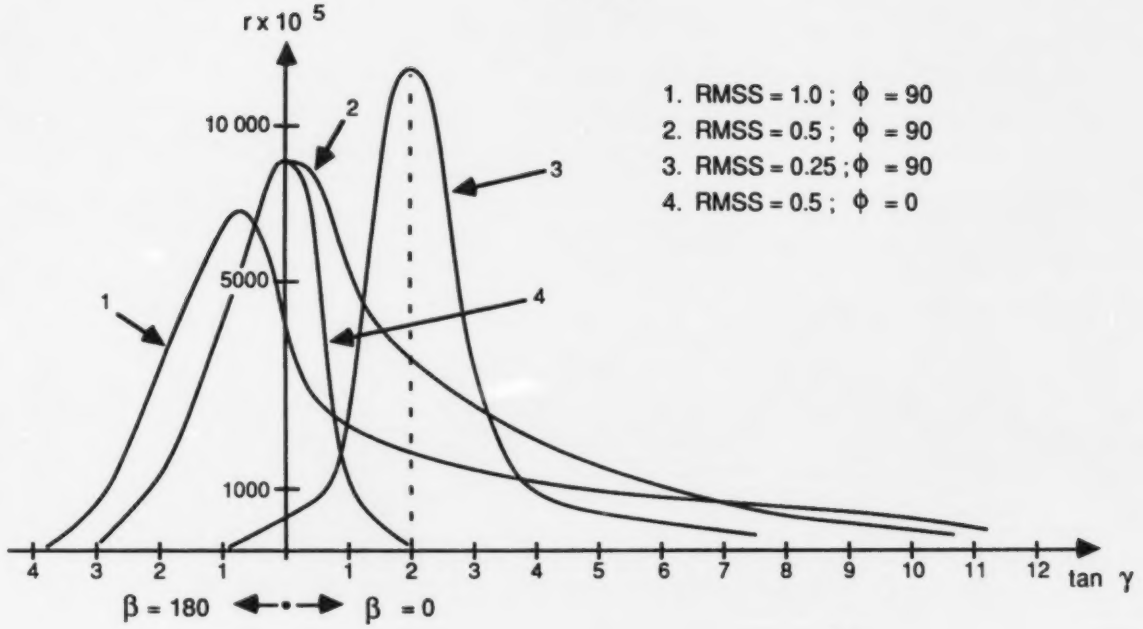

Figure 5 a/ Angular Characteristic of Light Scattering for Reflectance Angle of 30°

γ,β,ϕ Angles Defined on Figure 1

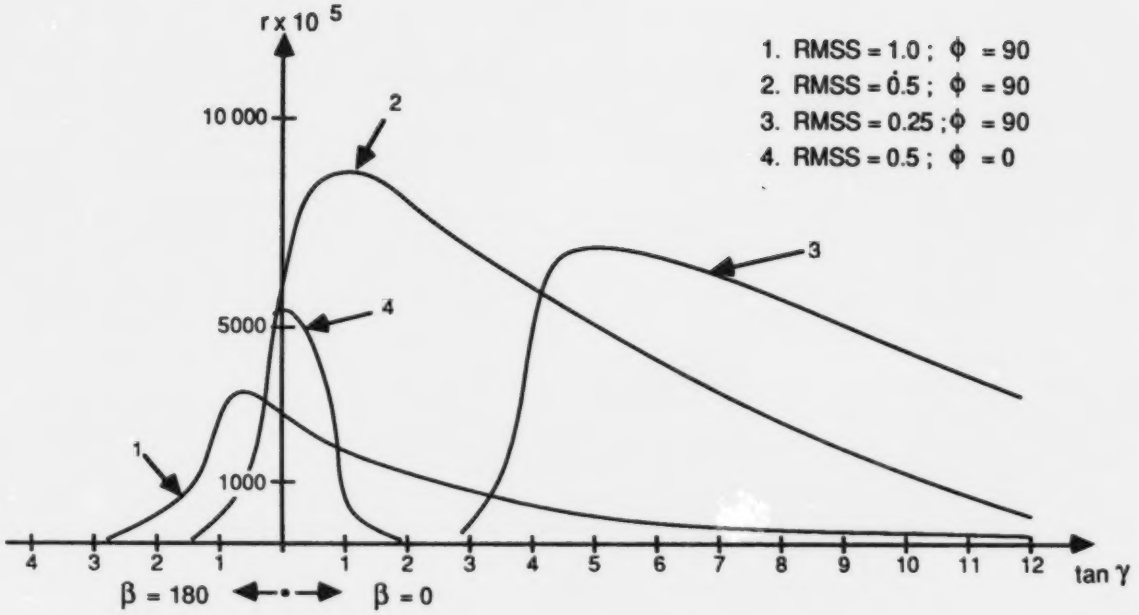

Figure 5 b/ Angular Characteristic of Light Scattering for Reflectance Angle of 1°;

γ,β,ϕ Angles Defined on Figure 1

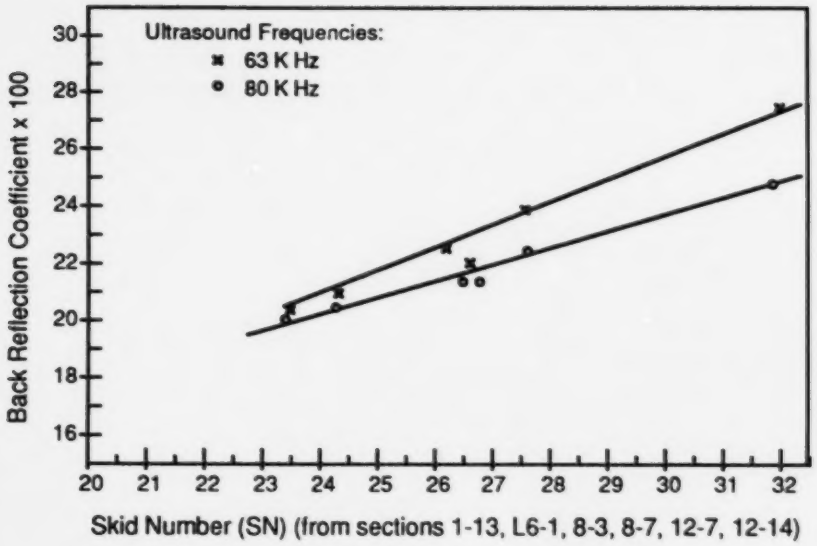

Figure 6/ Reflection of Ultrasound by Pavements of Different Roughness

REFERENCES

1. IES Roadway Lighting Committee, Proposed American National Standard Practice for Roadway Lighting, Journal of the Illuminating Engineering Society, April 1983, Volume 12, Number 3, pp. 146-196.

2. IES Roadway Lighting Committee, Proposed American National Standard Practice for Roadway Lighting, Journal of the Illuminating Engineering Society, April 1983, Volume 12, Number 3, pp. 146-196.

3. Jung, F.W., Kazakov, A.L., Titishov,A. Road Surface Reflectance Measurements in Ontario, In Transportation Research Record 996, TRB, National Research Council, Washington, D.C., 1984, pp. 24-37.

4. Jung, F.W., Kazakov, A.L., Titishov, A., Road Surface Reflectance Measurements in Ontario, Ontario Ministry of Transportation and Communications, Research and Development Branch, Canada, 1983.

5. Kazakov, A.L., A Model for Predicting the Reduced Reflectance Coefficient Matrix, Ontario Ministry of Transportation and Communications, Research and Development Branch, Canada, 1983.

6. Lord Rayleigh, The Theory of Sound, V.II, London, 1896.

7. Feinberg, E., On the Propagation of Radio Waves Along an Imperfect Surface, Journal of Physics, V.8, 6, pp. 317-330, 1944.

8. Rice S., Reflection of Electromagnetic Waves from Slightly Rough Surfaces, Com. Appl. Math., 4, pp. 351-378, 1951.

9. Brekhovskikh, L.M., Wave Diffraction at a Rough Surface, Journal of Experimental and Theoretical Physics, 3, pp. 275-304, 1952.

10. Isakovich, M.A., Wave Dispersion from a Randomly Uneven Surface, Journal of Experimental and Theoretical Physics, 23, 3(9), pp. 305-314, 1952.

11. Bass, F.G., Boundary Conditions for Average Electromagnetic Field on the Random Surface with the Random Fluctuation of the Impedance, Radiophysica, v.3, 1, pp. 72-78, 1960.

12. Kur'yanov, B.F., The Scattering of Sound at a Rough Surface with Two Types of Irregularities, Acoustics, V.8, 3, pp. 252-257, 1963.

13. Semyonov, B.I., Approximate Computation of Scattering of Electromagnetic Waves by Rough Surface Contours, Radiotechnica and Electronica, V.11, 8, pp. 1351-1361, 1966.

14. Beckmann, P.,and Spizzichino, A., The Scattering of Electromagnetic Waves from Rough Surfaces, New York, 1963.

15. Bass, F.G., Fuks, I.M., The Scattering of Waves from Random Rough Surfaces, Moscow, USSR, 1972, (in Russian).

16. Sancer,M.I., Shadow-Corrected Electromagnetic Scattering from a Randomly Rough Surface, IEEE Transactions on Antennas and Propogation, Vol AP-17, No. 5, Sept. 1969.

17. Stratton, J.A., Electromagnetic Theory, McGraw-Hill, N.Y., 1941.

18. Gutt,W., and Nixon, P.J., Studies of the Texture of Some Roadstone Materials by Scanning Electron Microscopy, Journal of Material Science, 7, pp. 995-1002, 1972.

19. Gradshtein, I.S. and Rijick, I.M., The Tables of Integrals, Sums, Series and Products, Moscow, Nauka, 1971, (in Russian).

20. Liebermann, L.N., Analysis of Rough Surfaces by Scattering, Journal of Acoustical Society of America, 35, 6, p. 932, 1963.

21. Kazakov, A.L., Blaney, C., The Scattering of Ultrasound by Pavement Surfaces, Ontario Ministry of Transportation and Communications, Research and Development Branch, Canada, 1985.

22. Osman, M.N., MTC Scale Model Facility for Transportation Noise Problems: Instrumentation Manual", June 1977, Ontario Ministry of Transpoprtation & Communications, R&D Branch, Report Number 77-AC-03.